ORIGINAL ARTICLE

Single-molecule optical mapping enables quantitative measurement of D4Z4 repeats in facioscapulohumeral muscular dystrophy (FSHD)

Yi Dai,[1] Pidong Li,[2] Zhiqiang Wang,[3] Fan Liang,[2] Fan Yang ![ORCID],[2] Li Fang,[4,5] Yu Huang,[6] Shangzhi Huang,[7] Jiapeng Zhou,[2] Depeng Wang,[2] Liying Cui,[1,8] Kai Wang ![ORCID] [4,5]

ABSTRACT

Purpose Facioscapulohumeral muscular dystrophy (FSHD) is a common adult muscular dystrophy. Over 95% of FSHD cases are associated with contraction of the D4Z4 tandem repeat (~3.3 kb per unit) at 4q35 with a specific genomic configuration (haplotype) called 4qA. Molecular diagnosis of FSHD typically requires pulsed-field gel electrophoresis with Southern blotting. We aim to develop novel genomic and computational methods for characterising D4Z4 repeat numbers in FSHD.

Methods We leveraged a single-molecule optical mapping platform that maps locations of restriction enzyme sites on high molecular weight (>150 kb) DNA molecules. We developed bioinformatics methods to address several challenges, including the differentiation of 4qA with 4qB alleles, the differentiation of 4q35 and 10q26 segmental duplications, the quantification of repeat numbers with different enzymes that may or may not have recognition sites within D4Z4 repeats. We evaluated the method on 25 human subjects (13 patients, 3 individual control subjects, 9 control subjects from 3 families) labelled by the Nb.BssSI and/or Nt.BspQI enzymes.

Results We demonstrated that the method gave a direct quantitative measurement of repeat numbers on D4Z4 repeats with 4qA allelic configuration and the levels of postzygotic mosaicism. Our method had high concordance with Southern blots from several cohorts on two platforms (Bionano Saphyr and Bionano Irys), but with improved quantification of repeat numbers.

Conclusion While the study is limited by small sample size, our results demonstrated that single-molecule optical mapping is a viable approach for more refined analysis on genotype-phenotype relationships in FSHD, especially when postzygotic mosaicism is present.

BACKGROUND

Facioscapulohumeral muscular dystrophy (FSHD) is a genetic disorder mainly affecting skeletal muscle. The disease progresses in a distinctive pattern and distribution. Clinical symptoms usually appear during the second decade. Weakness begins in the face, shoulders and upper arms, then followed by distal lower extremities, pelvic girdle and abdominal muscles. The symptoms often show marked asymmetry.[1] Several other extramuscular manifestations are also frequently observed in FSHD, with a high frequency of hearing loss (~75% patients) and retinal telangiectasia (60% patients),[2] as well as

defects in the central nervous system such as severe intellectual disability and epilepsy.[3] FSHD is the third most common form of muscular dystrophy and affects as high as 1 in 8,500 individuals in the Netherlands.[4] A significant variability in clinical expression is often observed, even among affected family members.

Two genetic subtypes of FSHD have been identified. The classical form, FSHD1, accounts for 95% of patients and is associated with a polymorphic macrosatellite repeat array on chromosome 4q35. The ~3.3 kb repeat unit is referred to as D4Z4, and patients typically carry 1–10 repeats, whereas non-affected individuals possess 11–150 repeats. Another D4Z4 repeat array on chromosome 10q26 exhibits almost complete sequence identity (~99%) to the 4q35 array.[5 6] Each D4Z4 repeat unit has a complex sequence structure, with several GC-rich repeat sequences and an open reading frame containing two homeobox sequences designated as double homeobox 4 (*DUX4*).[7 8] Both the 4q35 and 10q26 D4Z4 repeat arrays are highly polymorphic and exhibit extensive size variation in the normal population, but only the 4q35 repeats are associated with FSHD. A polymorphic segment of 10 kb directly distal to D4Z4 on 4q35 was identified,[9] with two alleles as 4qA and 4qB, and only the 4qA allele is pathogenic for FSHD.[10] *DUX4* transcripts within D4Z4 are efficiently polyadenylated and are more stable when expressed from 4qA background, suggesting that FSHD1 arises through a toxic gain of function attributable to the stabilised distal *DUX4* transcript.[11] A less common form, FSHD2, accounts for 5% of patients and is associated with the structural maintenance of chromosomes hinge domain 1 (*SMCHD1*) gene on chromosome 18p11.32.[12] In FSHD2, patients harbouring mutation in *SMCHD1* have a profound hypomethylation of chromosomes 4 and 10, allowing chromosome 4 to express the toxic *DUX4* transcript. Aberrant *DUX4* expression triggers a deregulation cascade inhibiting muscle differentiation, sensitising cells to oxidative stress and inducing immune responses and muscle atrophy.[13] A unifying pathogenic hypothesis for FSHD emerged with the recognition that the FSHD-permissive 4qA haplotype corresponds to a polyadenylation signal that stabilises the *DUX4* mRNA, allowing the toxic protein DUX4 to be expressed.[13]

109

Molecular diagnosis of FSHD is complicated by the relatively large size (~3.3 kb) and variable number of repeat units, the presence of homologous polymorphic repeat arrays on both chromosomes 4 and 10, as well as possible exchanges between these chromosomal regions. A Southern blot-based method, a BglII-BlnI dosage test, was developed to improve the sensitivity of conventional Southern blot for molecular diagnosis of FSHD.[14] The method was improved later using restriction enzyme Xap1 which complements Bln1, as the former uniquely digests repeat units derived from chromosome 4 and the latter uniquely digests those derived from chromosome 10.[15] After these developments, Southern blot could be used as a successful molecular diagnosis test of FSHD. However, the limitations of this method are evident: Southern blot needs four separate time-consuming enzyme/probe combinations and is semi-quantitative, since it estimates repeat count by size of a band in the gel and cannot assay very long alleles. Several attempts have been made to develop alternative methods for diagnosis of FSHD to overcome complications of Southern blot analysis, including molecular combing,[16 17] PacBio sequencing[18] and Nanopore sequencing.[19] Molecular combing has been used in the clinical context, and long-read sequencing in different platforms is also shown to be capable of determining the macrosatellite repeat number since they can generate reads that span over 100 kb regions.

In the current study, we aim to leverage a single-molecule optical mapping approach to characterise D4Z4 repeats in FSHD due to repeat contraction. This technique, also referred to as next-generation mapping, has been used for detection of structural variants (SVs),[20] and Barseghyan *et al* are among the first to use it in clinical settings, to identify pathogenic SVs in a series of patients diagnosed with Duchenne muscular dystrophy (DMD).[21] Unlike DMD, several key challenges in our study are the differentiation of 4qA alleles with 4qB alleles, the differentiation of 4q35 and 10q26 regions, the accurate quantification of repeat numbers and the ability to detect low levels of postzygotic mosaicism.

MATERIALS AND METHODS
Sample selection
Our primary patient cohort consists of five patients, including two from the same family (P02 and P03). Four of the patients have a family history of FSHD, but one patient (P04) is sporadic (table 1). All the patients had a molecular diagnosis of FSHD by Southern blots, and two of the patients were known to carry mosaicism based on Southern blots, although the exact fraction and the parental origin of the chromosome with postzygotic contraction cannot be determined. We stress here that the Southern blot and optical mapping on this cohort were blindly performed in two separate institutions without information from each other, yet the final results are consistent. Our second patient cohort consists of eight patients suspected to have FSHD, but without a prior molecular diagnosis. We performed Southern blot-based diagnosis on six patients with available DNA samples, as a validation assay after we obtained results from optical mapping. Additionally, existing data on two unaffected adult subjects without FSHD, as well as the publicly available data one individual and three families, were included in the study as negative controls.

Southern blot and PFGE-based DNA analysis
We followed previously published protocols for Southern blot.[10 22] All diagnostic testing by Southern blots were performed at the Department of Neurology, First Affiliated Hospital of the Fujian Medical University. For each sample, one portion of DNA samples was double digested with EcoRI/HindIII and with EcoRI/BlnI, yet another portion of DNA sample was digested only with HindIII. Then the digested DNA was separated by PFGE. After electrophoresis, the DNA was transferred to a Nytran XL membrane and hybridised with the probes p13E-11, 4qA, 4qB, respectively. Finally, the blots were exposed to obtain images for further manual analysis of repeat numbers.

High molecular weight (HMW) DNA isolation for optical mapping
Fresh blood samples were collected in EDTA-stabilised anticoagulative tube, adequately mixed and stored at 4°C promptly. Samples that cannot be processed within 5 days after collection were stored at −80°C. HMW DNA was extracted from either 1 mL frozen or fresh blood, following manufacturer's guidelines (Bionano Prep Blood DNA Isolation Protocol, Bionano Genomics, #30033) with slight modifications. Briefly, red blood cells (RBCs) were lysed by RBC lysis solution (Qiagen) and white blood cells (WBC) left were pelleted. After centrifugation, WBC were resuspended in cell buffer (Bionano Genomics, USA), and then the WBC solutions were embedded into 2% agarose plugs (CHEF Genomic DNA Plug Kit, Bio-Rad) to avoid fragmentation of long DNA molecules, with overnight lysis at 50°C in lysis buffer (Bionano Genomics) with Puregene Proteinase K (Qiagen). The volume ratio (v/v) of WBC and agarose were typically 1.5:1, 2:1, 4:1, 8:1 and 16:1, in order to obtain DNA with proper concentration. (We typically do a quick DNA extraction before embedding the cells into the plug, and we choose a ratio that yields ~2.2 μg DNA per plug which corresponds to approximately 6×10^5 cells.) The agarose plugs were washed with Tris-EDTA buffer the following day and digested at 43°C with GELase Agarose Gel-Digesting Prep (2 unit/μL, Thermo Fisher) for 50 min. Extracted HMW DNA was purified via drop dialysis using Millipore membrane filters (EMD Millipore, USA) placed on Tris-EDTA buffer for 3 hours.

DNA quantification was carried out using Qubit dsDNA assay BR kits with a Qubit 2.0 Fluorometer (ThermoFisher Scientific). The integrity of HMW DNA was detected by PFGE (Pippin Pulse, Sage Science). Only the DNA samples with concentration between 30 and 100 ng/μL and sufficient molecular mass were used in the following DNA labelling experiment.

DNA labelling and CHIP loading
The DNA labelling experiment (also referred to as 'NLRS') consists of four sequential steps (nick, label, repair and stain), and was performed strictly following manufacturer's guidelines (Bionano Prep Labelling—NLRS Protocol, Bionano Genomics, #30024). In short, 300 ng of purified HMW DNA was nicked by nicking endonucleases Nb.BssSI (New England BioLabs) in 10× Buffer 3.1 (Bionano Genomics) at 37°C for 2 hours. Using Taq polymerase (New England BioLabs), the nicked DNA was labelled at 72°C for 1 hour by fluorophore-labelled nucleotides mixed in 10× Labelling mix (Bionano Genomics). In the third step, labelled DNA was repaired with Taq ligase (NEB) at 37°C for 30 min to restore integrated double strands DNA. In the last step, the DNA backbone was stained overnight in a dark environment at 4°C for visualisation and size identification. DNA quantification was carried out using Qubit dsDNA assay HS kits with a Qubit 2.0 Fluorometer (ThermoFisher Scientific) and only DNA samples with concentration between 4 and 10 ng/μL were chosen to be loaded in the next step.

Table 1 A list of patients and control subjects assayed by the Bionano Saphyr platform in the current study. More detailed description of results can be found in online supplementary table 1

	ID	Sex	Age (years)	Onset (years)	Family history	CK (U/L)	EMG	Southern blot (4q35) Length (kb)	Units	Allele	Optical mapping (Nb.BssSI enzyme, 4q35) Units	Allele	Read count	Optical mapping (Nt.BspQI enzyme, 4q35) Units	Allele	Read count
Patient cohort 1	P01	F	37	28	+	104	Mild myopathic change	~20	~4	4qA	4	4qA	6	4.3±0.3	4qA	38
								~38	>10	4qB	22	4qB	5	22.4±0.2	4qB	23
	P02	F	18	12	+	379	Myopathic change	~18	~3	4qA	3	4qA	25	–	–	–
								~98~	~28	4qA	28	4qA	10	–	–	–
	P03	F	43	30	+	110	Mild myopathic change	~18	~3	4qA	3	4qA	27	–	–	–
								~38	>10	4qA	11	4qA	34	–	–	–
	P04	M	27	11	–	1406	Myopathic change	~16	~3	4qA	3	4qA	18	–	–	–
								~61	~17	4qB	19	4qB	42	–	–	–
								~76	~21	4qA	23	4qA	30	–	–	–
	P05	F	41	31	+	95	Normal	~12	~2	4qA	2	4qA	12	–	–	–
								~38	~10	4qA	11	4qA	18	–	–	–
								>38	>10	4qA	17	4qA	60	–	–	–
Patient cohort 2	P06	F	14	6	–	406	Myopathic change	–	–		2	4qA	3	2.2±0.3	4qA	32
											15	4qB	4	15.0±0.2	4qB	36
											27	4qA	3	27.2±0.4	4qA	5
	P07	M	23	18	–	871	Myopathic change	–	–		4	4qA	6	–	–	–
								–	–		20	4qA	11	–	–	–
	P08	M	18	13	–	538	Myopathic change	~21.5	~5	4qA	5	4qA	6	–	–	–
								>63.5	>17	4qA	25	4qA	9	–	–	–
	P09	F	33	19	–	269	Mild myopathic change	~21.5	~5	4qA	5	4qA	33	–	–	–
								>63.5	>17	4qA	18	4qA	26	–	–	–
	P10	F	39	28	–	176	Myopathic change	~15	~3	4qA	3	4qA	17	–	–	–
								>63.5	>17	4qA	28	4qA	8	–	–	–
	P11	M	20	14	+	379	Myopathic change	~15	~3	4qA	3	4qA	16	–	–	–
								>63.5	>17	4qA	32	4qA	12	–	–	–
	P12	F	15	10	–	514	No data	~12	~2	4qA	2	4qA	10	–	–	–
								~48.5	15	4qA	16	4qA	18	–	–	–
	P13	F	53	32	+	341	Myopathic change	~18.5	~4	4qA	4	4qA	18	–	–	–
								>63.5	>17	4qB	18	4qB	18	–	–	–
Control	C01	F	–	–	–	–	–	–	–		19	4qB	8	18.8±0.3	4qB	22
											47	4qA	10	46.5±0.5	4qA	13
	C02	M	–	–	–	–	–	–	–		18	4qA	8	18.6±0.3	4qA	7
											20	4qA	9	20.5±0.1	4qA	8
	C03	M	–	–	–	–	–	–	–		13	4qB	4	12.7±0.5	4qB	20
											22	4qB	4	22.2±0.4	4qB	22

More detailed description of results can be found in online supplementary table 1.
CK, creatine kinase; EMG, electromyography; F, female; M, male.

Labelled DNA was loaded on the Saphyr chip and pushed by low-voltage electric field into pillar region and nanochannel in the Bionano Saphyr instrument. After the mapping procedure begins, the fluorescently labelled DNA molecules were imaged by the Saphyr instrument. Generally, after 24–36 hours, each sample can generate 320–480 Gb data for each flow cell, which was used for further data analysis.

Downloading data sets from publicly available resources

The data sets on the NA12878 genome were downloaded from Bionano Genomics's website (https://bionanogenomics.com/library/datasets/). The data sets of the three family trios in the 1000 Genomes Project were provided by Bionano Genomics.

Bioinformatics approaches to analyse optical mapping data

The detailed description of the bioinformatics algorithms is provided below. In particular, we addressed the challenges in the differentiation of 4qA with 4qB alleles, the differentiation of 4q35 and 10q26 segmental duplications, the quantification of repeat numbers with different enzymes that may or may not have recognition sites within D4Z4 repeats.

Data preprocessing and alignment

The raw output files from the Bionano Saphyr mapping platform and Irys platform were in BNX formats. Each file contained molecule and label information and quality scores per channel identified during a Bionano run. Where necessary, for each subject, we combined several BNX files into one BNX file. We next performed a basic filtering of the BNX file using all default parameters suitable for human genome, including the 150 kb length cut-off and the label SNR filter. To assess the quality of each of the Bionano runs, we performed Molecular Quality Report using default parameters and examined the results by comparing with manufacturer-recommended values. Additional details can be found at https://bionanogenomics.com/wp-content/uploads/2017/05/30175-Rev-A-Bionano-Molecule-Quality-Report-Guidelines.pdf

For each enzyme, we performed in silico digestion of the human reference genome (GRCh38) to generate the reference map for that particular enzyme (ie, the reference CMAP file). We then mapped the BNX files to the reference CMAP file, using the Bionano-Solve (V.3.1), accessed from https://bionanogenomics.com/support/software-downloads/. Slight modifications were made to the source code align_bnx_to_cmap.py to change all the hard-coded path names in the software. The results include three file types: xmap, r.cmap and q.cmap. They represent the alignment file, the reference label file and the query label file, respectively. A custom script was developed to extract specific regions of alignments from whole-genome mapping to speed up subsequent data analysis and visualisation.

Determination of repeat copy number and 4qA/4qB configuration by Nb.BssSI enzyme

We developed a simple yet effective approach for quantifying repeat units and determining 4qA/4qB configurations using Nb.BssSI-based labels. Through the analysis of an empirical mapping data set on human samples, which was already normalised through a scaling factor to account for the variation of DNA migration rates during Bionano data acquisition, we calculated that the length of D4Z4 repeat unit (hereafter referred to as r) is 3299.4 ± 144.00 bp (mean±SD), the distance of 4qA to the D4Z4 repeat unit (hereafter referred to as q) is 1758.79 ± 61.15 bp and the distance to the first label

immediately after 4qA to the 4qA label (hereafter referred to as s) is 7889.79 ± 240.93 bp. These observations suggest that the three measures (r, q, s) are quite distinct from each other and their variances are small enough so that they can be easily differentiated in real data. Based on these empirical observations, we set a coefficient of variation (hereafter referred to as t) upper bound of 0.05, which is a measure of relative variability as the ratio of the SD to the mean (the empirical observations had t values of 0.044, 0.035 and 0.031 for the three measures, respectively).

Our algorithm accounts for the relatively high error rates in the label data. Based on technical documentation from Bionano (https://bionanogenomics.com/wp-content/uploads/2017/05/30175-Rev-A-Bionano-Molecule-Quality-Report-Guidelines.pdf), the percentage of unaligned labels in molecules relative to number of labels in molecules and the percentage of unaligned reference labels relative to number of reference labels are generally <15% and 21%, respectively, for a mapping data set with reasonable quality. Our algorithm first examines reads that are mapped to the 4q35 target region (figure 2) with sufficient number of labels in the 'region of dissimilarity' to ensure that the reads originate from 4q35 rather than 10q26. For each read, we denote the position of the first label within D4Z4 region as l_1 for simplicity, and all following labels as l_2, l_3 up to l_n (the last label in the read). We then calculate a distance vector between all adjacent labels as $d = [d_1, d_2, d_3, \ldots, d_{n-1}] = [l_2 - l_1, l_3 - l_2, l_4 - l_3, \ldots, l_n - l_{n-1}]$. Based on each d_i ($1 \leq i \leq n-1$) in the vector, we classify each label into one of five categories of events: (1) one additional D4Z4 repeat, when $r(1-t) \leq d_i \leq r(1+t)$; (2) one or two false-negative labels (ie, expected label is missing from reads), when $r(1+t) < d_i \leq 3r(1+t)$; (3) one or two false-positive labels (ie, extra label is present in reads), when $r(1-t) < d_i + d_{i+1} \leq r(1+t)$ for one extra label, or when $r(1-t) < d_i + d_{i+1} + d_{i+2} \leq r(1+t)$ for two extra labels; (4) 4qA is encountered, when $q(1-t) \leq d_i \leq q(1+t)$ and when $s(1-t) \leq d_{i+1} \leq s(1+t)$; (5) a label outside of D4Z4 repeat region is encountered, or an exception is encountered when the first four criteria are not met. Optionally, the prior probability for the five events can be determined from genome-wide estimate of false-positive and false-negative rates when mapping all reads to the reference genome GRCh38, to assign reads into the five categories based on posterior probability. When more than one consecutive category 5 events are encountered, the label counting for this read ends and the number of estimated repeat counts is recorded. For each sample, the results for all reads are then tallied in a histogram. A peak-calling algorithm is used to classify one peak (homozygous, which is rare), two peaks (heterozygous) or three peaks (postzygotic mosaicism), and quantify the number of repeat units corresponding to each peak. We also note that although we have not encountered this situation in practice, it is possible that all reads spanning this region have only category 5 events, when the patient carries zero copies of D4Z4 repeat units in both alleles.

Determination of repeat copy number and 4qA/4qB configuration by Nt.BspQI enzyme

Although less straightforward, we also developed a simple yet effective approach for quantifying repeat units and determining 4qA/4qB configurations using Nt.BspQI-based labels. Based on the published sequence of D4Z4 (GenBank: D38024.1),[23] we determined the position of D4Z4 repeat units on 4q35 in the human reference genome GRCh38 as shown in online supplementary table 4 (we note that a previous study[24] incorrectly determined repeat units in GRCh38). However, with

one possible exception, analysis of a large number of real data sets failed to detect Nt.BspQI labels in repeat unit #2 and #5, suggesting that GRCh38 may have included a very rare allele or may contain assembly errors in this region. Similarly, we determined the position of D4Z4 repeat units on 10q26 (online supplementary table 5) and on KQ983257.1 (online supplementary table 6), and illustrated the presence of a genome assembly gap on 10q26 that incorrectly created two separate repeat arrays in GRCh38 (GRCh37 is not influenced by this issue as shown in figure 2).

Based on in silico enzyme digestion of GRCh38 by the Nt.BspQI enzyme, we found that there is a restriction enzyme recognition site 7271 bp upstream of the first D4Z4 repeat unit in GRCh38 (CMAP coordinate as chr4: 190058870), and that there is another restriction enzyme recognition site 7860 bp downstream of the last D4Z4 repeat unit in GRCh38 (CMAP coordinate as chr4: 190100364). Therefore, when we can anchor a read to the two enzyme recognition sites, we can calculate the distance between two labels as x, and estimate the number of D4Z4 repeat units as $y = (x - 7271 - 7860)/3300$. Unlike our analysis on Nb.BssSI, the estimate y here is a floating point value rather than an integer. When multiple reads are mapped to the same region, we can calculate the value of y to yield a best estimate of the number of repeat units. As previously discussed,[24] based on empirical evidence, the 4qA and 4qB configuration can be differentiated by the presence of five labels (4qA) or three labels (4qB) downstream of D4Z4 repeat region.

Visualisation and manual examination of results

We used the Bionano Access software for visualisation of genome mapping and manual examination of results. The software was obtained from https://bionanogenomics.com/support-page/bionano-access/. It is a node.js web application that can communicate with a remote server, but can also run in standalone mode to perform visualisation of results.

We extracted a subset of reads that mapped to 4q35 and 10q26 regions and performed manual examination of their alignment. The results are generally consistent with computational results, further suggesting that the method is highly reliable.

RESULTS

Optical mapping on long DNA molecules can differentiate paralogous genomic regions

Optical mapping[25] is a technique for mapping locations of restriction enzyme sites in DNA molecules. In the current study, we applied a high-throughput platform, the Bionano Saphyr Genome Mapping platform, to perform optical mapping on high molecular weight (HMW) (>150 kb) DNA molecules. The presence of highly similar D4Z4 repeat units in both 10q26 and 4q35 chromosome regions complicates the genome mapping of DNA molecules originating from these regions. To illustrate this, we plotted the genomic regions that contain the D4Z4 repeat units (DUX gene clusters) in 4q35 and 10q26 (figure 1A and B). Only the cluster in 4q35 are related to the development of FSHD, when there is a contraction of copy number of the D4Z4 repeat units in this cluster. Furthermore, a polymorphic segment of 10 kb directly distal to D4Z4 on 4q35 carry two different allelic configurations in the population, commonly referred to as 4qA and 4qB, and only the 4qA allele is pathogenic for FSHD.[10] An additional variant of 4qA allele is the 4qA-L allele, with a slightly longer D4Z4 unit at the most distal end.

In the GRCh38 reference genome, 4q35 carries two D4Z4 arrays interrupted by a 50 kb gap, one array with 4qB

configuration (8 D4Z4 repeat units) and one array with a 4qA configuration (1.5 D4Z4 repeat units). The GRCh38 reference sequence of 10q26 shows two 7 unit D4Z4 arrays with a 10q configuration and an incorrect 50 kb gap in between. This should be a single continuous D4Z4 array on both chromosomes. Recently, a new scaffold covering this region was incorporated into GRCh38 patch 7 (KQ983257.1) without the gap, and we additionally illustrated the segmental duplication in this 230 kb scaffold, which has a 4qA configuration with 13 D4Z4 repeats (figure 1C). At the same time, a new scaffold representing the 4qA-L allele was incorporated into GRCh38 patch 7 (KQ983258.1) without the gap (figure 1D). We note that GRCh37 does not contain this mistake and shows the correct chromosome 4 and 10 assemblies, but it has a 4qB configuration in chromosome 4 (figure 1E and F). In summary, successful molecular diagnosis of FSHD requires accurate quantification of D4Z4 repeats within the 4q35 region with high specificity, and the differentiation of the 4qA and 4qB alleles.

Determining D4Z4 repeat copy number on 4q35 by Nb.BssSI enzyme labelling

We initially selected the Nb.BssSI restriction enzyme for the study, since each D4Z4 unit contains a recognition site for this enzyme, as previously suggested.[24] Through the analysis of fluorescence labels generated by in silico digestions with the Nb.BssSI enzyme, we have identified the regions of label similarity and dissimilarity between the paralogous genomic regions on chromosomes 4q35 and 10q26 (figure 2). Our computational analysis showed that when a DNA molecule is long enough to stretch out into the region of dissimilarity (figure 2, blue box), we can determine whether the molecule originates from 4q35 or 10q26. Furthermore, when using Nb.BssSI enzyme, based on the presence or absence of one additional label ~1.8 kb distal to the last label in the D4Z4 repeat regions, we can determine the allelic configuration to be 4qA or 4qB.

We evaluated this approach on five patients who were well characterised clinically (table 1, online supplementary table 1). All of them had a positive diagnosis of FSHD through Southern blot (figure 3), and two of them (ID: P04 and P05) were known to carry postzygotic mosaicism (as denoted by the '+' sign in figure 3). The analysis of mapped reads confirmed the presence of contracted alleles in all five patients (table 1, online supplementary table 2). We illustrate the observed label patterns on all patients in online supplementary figure 2, where the presence of fluorescence labels can be easily and directly visualised and counted in the Bionano Access browser. Although some enzymatic labels appear to be missing given the imperfect labelling efficiency of the enzyme, it is possible to computationally predict the missing labels based on distances between neighbouring labels representing D4Z4 repeats (see 'Materials and methods' section). When multiple reads are piled at the same locus, each read will be assigned an estimated repeat count, and a peak-finding algorithm was used to identify the presence of peaks and yield an estimate of the repeat counts.

We next examined whether our methods can detect the presence of postzygotic mosaicism on 4q35, since two patients were known to carry mosaicism from Southern blot. For example, for a patient (ID: P04), the presence of fluorescence labels can be directly visualised and counted in the Bionano Access browser, with 3, 19 and 23 repeats and the number of supporting reads as 18 (20%), 42 (46.7%) and 30 (33.3%), respectively. Since the three alleles were in 4qA, 4qB and 4qA configurations, respectively, we speculate that the allele with 3 repeats was due to a
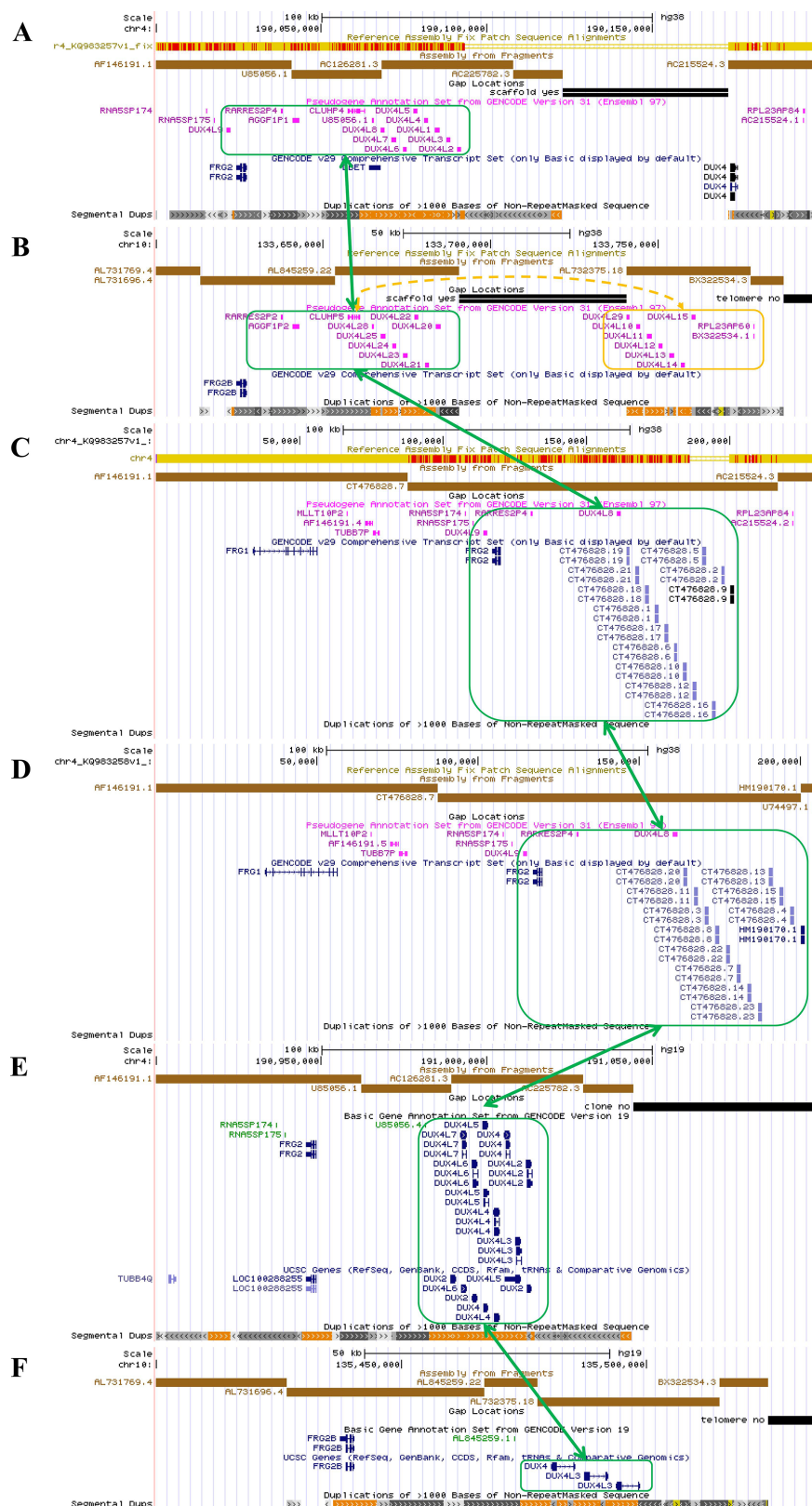
Figure 1 An overview of the genomic architecture of segmental duplications at the chromosome 4q35 region and the 10q26 region. In the GRCh38 reference genome, 4q35 incorrectly shows two D4Z4 arrays (8 units 4qB type and 1.5 unit 4qA type) with a 50 kb gap between AC225782.3 (4qB) and AC215524.3 (4qA) (panel A). 10q26 incorrectly shows two D4Z4 arrays (each with 7 D4Z4 repeat units) with a 50 kb gap between AL845259.22 (10qA) and AL7323751.8 (10qA) (panel B). Two new patch scaffold sequences were recently added in CRCh38 patch 7 with 4qA configuration (KQ983257.1) without gap and with 4qA-L configuration (KQ983258.1) without gap, and we additionally illustrated them (panel C and D). The segmental duplication (green boxes) in 4q35 has high sequence identity with the corresponding region in 10q26, KQ983257.1 and KQ983258.1, while the distal D4Z4 array separated by the gap in 10q26 is marked with an orange box. The incorrect assembly gap is not present in 4q35 (panel E) or 10q26 (panel F) in the GRCh37 genome assembly.
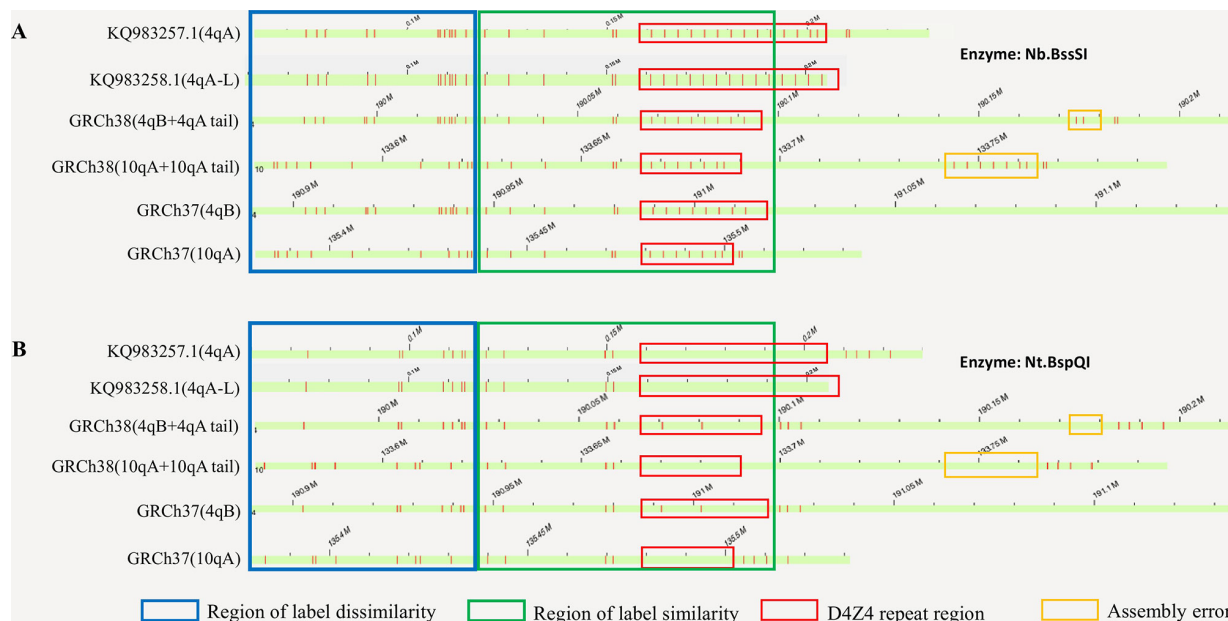
Figure 2 Illustration of the region with label dissimilarity between 10q26, 4q35, KQ983257.1 and KQ983258.1 (blue box) adjacent to the region of similarity (green box), based on in silico analysis on GRCh37, GRCh38, KQ983257.1 and KQ983258.1. Red vertical bars represent labels of enzyme recognition sites. By using fragments that spans the region of dissimilarity, we can confidently separate fragments originating from 10q26, 4q35 or those that are undetermined (uninformative). The panel A and B represent labels generated by the Nb.BssSI and Nt.BspQI enzymes, respectively. Although the reference genome GRCh38 contains two labels (repeat unit #2 and #5) within the D4Z4 repeat region for the Nt.BspQI enzyme (red box), we rarely observe them in real data, possibly due to the inclusion of a very rare allele in the GRCh38 or due to errors in genome assembly.

postzygotic contraction of D4Z4 repeat units from the allele with 23 repeats, resulting in disease manifestation. We acknowledge that the read counts may be biased by the length of the reads and

by the performance of the alignment algorithm. Furthermore, we also noticed that the repeat counts for the longer allele in P04 and P05 are slightly different (±1–2 repeats) from those
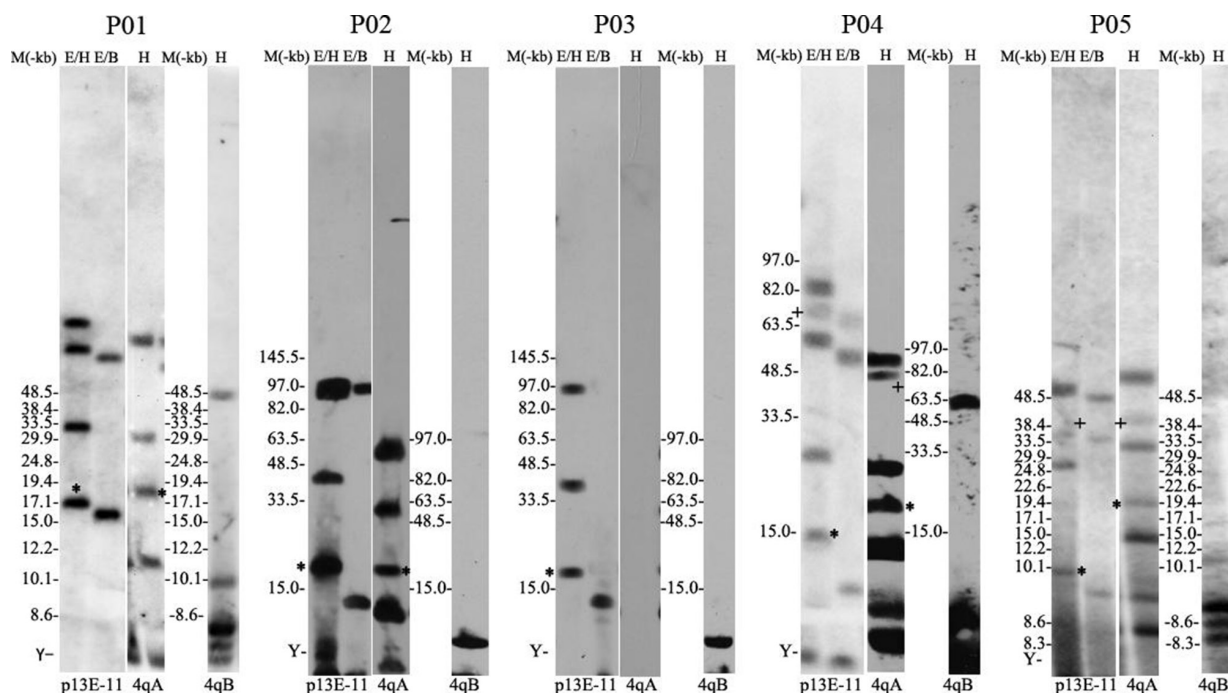

Figure 3 Molecular diagnosis of facioscapulohumeral muscular dystrophy by Southern blot on samples from cohort 1. The results for cohort 2 is available in online supplementary figure 1. E/H and p13E-11: double digested with EcoRI/HindIII and then labelled with probe p13E-11, and all the 4q and 10q segments are illustrated. E/B and p13E-11: double digested with EcoRI/BlnI and then labelled with probe p13E-11, and the 10q segments are digested so only 4q segments are illustrated. H and 4qA: digested with HindIII and then labelled with probe 4qA, and the 4qA alleles are illustrated. H and 4qB: digested with HindIII and then labelled with probe 4qB, and the 4qB alleles are illustrated. The asterisk '*' denotes pathogenic allele with <10 repeat units and with a 4qA configuration. The plus sign '+' denotes somatic mosaic allele.

inferred by Southern blot. Since Southern blot estimates repeat counts by band size in a gel, for alleles with larger number of repeats, it may be less quantitative than direct visualisation of labels in optical mapping, and it cannot measure very long alleles (typically represented as more than a threshold such as '>38 kb' or '>10 repeats' in diagnostic reports).

Determining D4Z4 repeat copy number on 4q35 by Nt.BspQI enzyme labelling

Most published and ongoing human genetics studies use Nt.BspQI on the Bionano platform, partly due to its robustness and high sensitivity to recognise DNA motifs. Therefore, it would be ideal to develop methods that can use this enzyme as well, to determine the copy number of D4Z4 repeat units. Our in silico digestion analysis on the reference genome GRCh38 demonstrated that it is possible to differentiate reads originating from 4q35 and 10q26 (figure 2B). Although the reference genome GRCh38 contains two Nt.BspQI labels within the D4Z4 repeat region, we do not observe them in real data, possibly due to the inclusion of a very rare allele or due to genome assembly errors in GRCh38. Instead, based on recognition sites surrounding the D4Z4 repeat array, we can infer the length of the D4Z4 array purely based on the distance between flanking regions with fluorescence labels (figure 2B). Note that even if a very rare allele does include enzyme recognition site within the D4Z4 repeat, it will not negatively impact our calculation, as our method estimates the length of the repeat based on fluorescence label pattern of the flanking regions. Additionally, although the human reference genome GRCh38 contains one array with 4qB configuration (8 D4Z4 repeat units) and one short array with a 4qA configuration (1.5 D4Z4 repeat units), our empirical analysis and previous report[24] demonstrated that the 4qA/4qB allele type of the repeat units can be confidently assigned by the presence of a 5-label or 3-label array distal to the D4Z4 repeat array. We additionally note that the 4qA sequence was recently added into CRCh38 patch 7 (KQ983257.1), as illustrated in figures 1 and 2. Furthermore, the patch also includes the variant 4qA-L haplotype (KQ983258.1), which is Caucasian-specific and is slightly longer than the 4qA haplotype, as illustrated in figure 1.

To further examine this possibility, we performed optical mapping on selected patients using the Nt.BspQI enzyme. For example, for the patient (ID: P01) in online supplementary figure 2, the distance between two flanking segments of the D4Z4 clusters can be used to quantify the number of repeats. Unlike our analysis using the Nb.BssSI enzyme where the enzyme recognition site is directly located within the D4Z4 repeat unit, we can assign a quantitative (floating-point) repeat count to each DNA molecule that spans the region of dissimilarity, since the enzyme recognition sites are outside of the repeat regions. The information from all reads can be compiled together to reach an estimate of the repeat counts for both alleles (4 and 22 repeats, respectively), and our results were completely consistent with the results obtained from the Nb.BssSI enzyme.

Additional validation on a second patient cohort and on control subjects

To further validate the method in diagnostic testing settings, we analysed a second cohort of eight individuals suspected to have FSHD, from two separate institutions. These patients all had typical clinical manifestations consistent with FSHD (table 1). However, they were not previously subject to any diagnostic testing of FSHD. We performed the genetic analysis on the Bionano Saphyr single-molecule optical mapping platform. We

obtained positive results on all the patients, and found that one patient (ID: P06) had postzygotic mosaicism with 2, 15 and 27 repeats (figure 4). We validated this result using both the Nb.BssSI enzyme and Nt.BspQI enzyme. Since the allele with 15 and 27 repeats had 4qB and 4qA configuration, respectively, we can further infer that the postzygotic contraction of D4Z4 repeats occurred on the allele with 27 repeats in 4qA configuration, which represented a dramatic decrease of D4Z4 copy number on this allele. Finally, we obtained Southern blot-based diagnosis from an independent diagnostic lab on six individuals for whom sufficient DNA is available (online supplementary figure 1). The estimated repeats from Southern blot are highly consistent with those inferred from optical mapping (table 1, online supplementary table 2).

In addition to patient cohorts, we evaluated our approach on several control subjects without FSHD and without a family history of FSHD. We also downloaded publicly available Bionano genome mapping data sets on the NA12878 subject (ID: C01). The results from both the Nb.BssSI enzyme and Nt.BspQI enzyme were consistent with each other for all the subjects (table 1), suggesting that the method can work on healthy human populations with larger number of D4Z4 repeat units.

Finally, we evaluated whether our method can be applied to an earlier generation of the single-molecule optical mapping platform, the Bionano Irys platform. We performed additional analysis on three control families from the 1000 Genomes Project (table 2). With one exception (family 1), we found that the D4Z4 repeat unit numbers and allelic configuration of the offspring and the parents in all three families were consistent with Mendelian inheritance, demonstrating high accuracy of the method. However, the discrepancy of the allelic configuration on family 1 highlighted the potential problem with the earlier generation of the optical mapping platform, which has lower throughput (thus lower coverage) and generally shorter fragment sizes, and that assessment of repeat number and allelic configuration may be susceptible to calling errors when <10× coverage is obtained. Additionally, the results from the Nb.BssSI enzyme and Nt.BspQI enzyme were also consistent with each other, except for three subjects who carried large unit numbers. However, we also note that for three subjects, only one allele was quantified using the data sets of Nb.BssSI enzyme, but both alleles can be quantified using the data sets of Nt.BspQI enzyme. Additionally, the 4qA/4qB configuration for one subject is different between the results generated by the Nt.BspQI enzyme and Nb.BssSI enzyme. The largest number of units detected in our study is 49. Thus, we caution that optical mapping on the older Irys platform may be less effective for human subjects carrying >50 D4Z4 repeat units, given the size limitations of typical DNA extraction and optical mapping experiments on the Irys platform. In summary, we caution that the Irys platform may limit the performance, due to generally lower throughput (lower coverage) and shorter DNA fragments during DNA preparation, and may generate incorrect 4qA/4qB allelic configurations.

DISCUSSION

In this study, we evaluated the technical feasibility of using nanochannel-based optical mapping to characterise D4Z4 repeat numbers and allelic configurations in FSHD. We demonstrated that this method can accurately quantify the number of repeats, can differentiate the DNA fragments from 4q35 and 10q26 and can quantify the mosaic levels of repeats when one allele has a postzygotic contraction of D4Z4 repeat units. We concluded
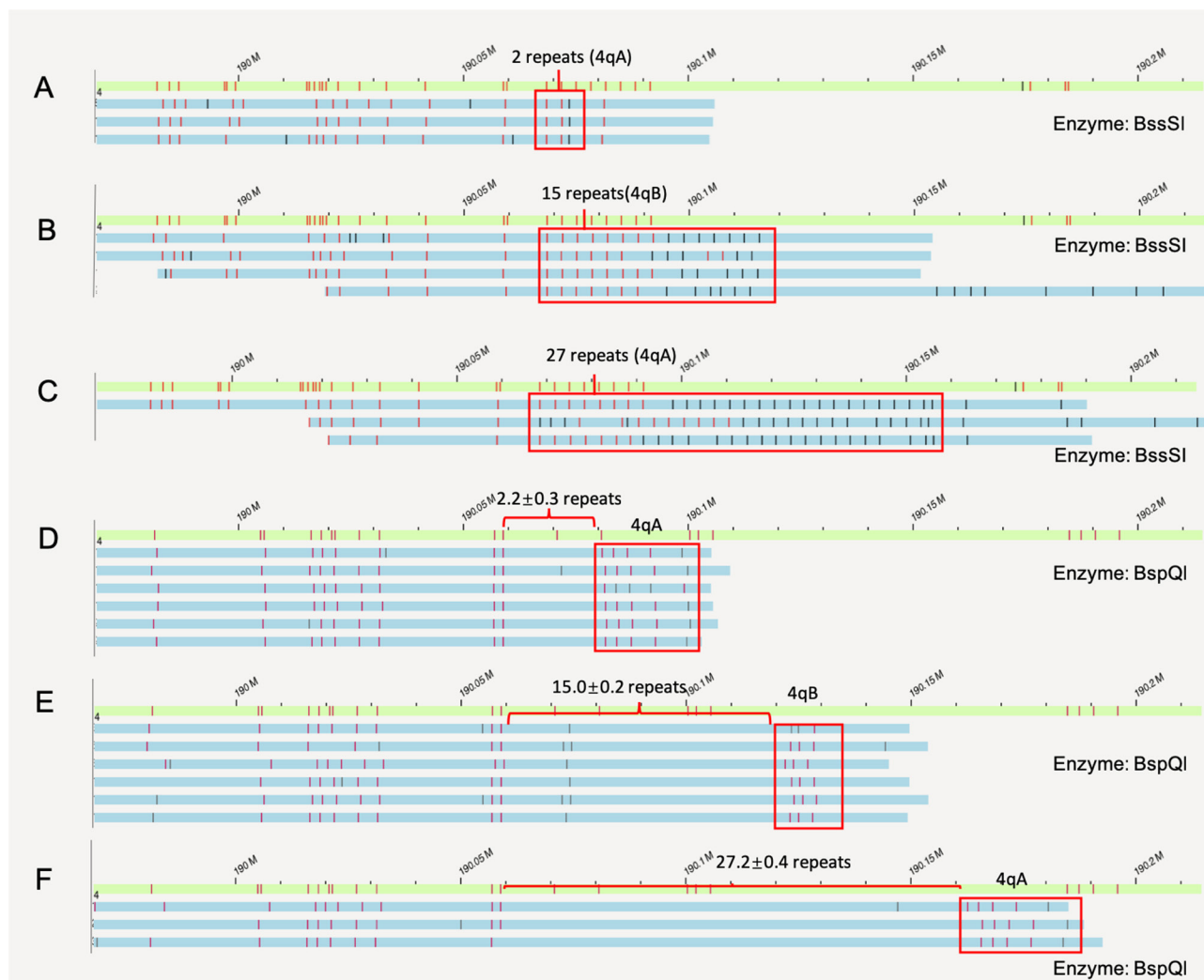
Figure 4 Determination of somatic mosaicism by Nb.BssSI (panel A/B/C) and Nt.BspQI (panel D/E/F) enzymes on a patient with 2, 15 and 27 repeats (ID: P06). For both enzymes, our computational pipeline accurately identified the presence of somatic contraction, and determined that the contraction occurs on the parental allele carrying the 4qA configuration. For repeat quantification using the Nt.BspQI enzyme, mean±SD is annotated in the figure. Vertical bars represent labels of enzyme recognition sites.

that optical mapping is a viable approach for quantifying D4Z4 repeats in FSHD and may be applied in clinical diagnostic settings once more validations are performed in the future.

Compared with conventional optical mapping approaches, the nanochannel-based optical mapping has several clear advantages. First, by stretching the DNA molecules as linear molecules and going through massively parallel nanochannels, the resolution and throughput are much higher than conventional optical mapping approaches that spread labelled DNA molecules on glass slides in semi-controlled fashion. Additionally, when Nb.BssSI enzyme is used, the labels (one for each D4Z4 unit) can be directly visualised in optical mapping platform. As illustrated in a previous study using optical mapping on FSHD,[26] the ability to visually check and count repeats is a major advantage over Southern blot and FISH combing. A second advantage is the flexibility to switch to different enzymes to allow detection of different patterns. In our study, we demonstrated that Nb.BssSI enzyme is a preferred choice for FSHD since an enzyme recognition site is directly located within the D4Z4 repeat unit, but we also developed methods to quantify the repeat number with the Nt.BspQI enzyme labelling. Recently, molecular combing is also used to detect the copy number of D4Z4 repeat units.[16]

However, molecular combing only detects the approximate length of the D4Z4 array and the repeat number is inferred from the length. In comparison, we can calculate repeat numbers directly using the Nb.BssSI enzyme, while also estimate the length of D4Z4 array using the Nt.BspQI enzyme in a similar fashion as molecular combing. We also recognise that long-read sequencing technologies, such as PacBio single-molecule real-time sequencing and Oxford Nanopore sequencing, may also be used in the molecular diagnosis of FSHD. However, these sequencing techniques usually produce data with read length N50 <20 kb. Ultra-long nanopore sequencing with a special library construction procedure may produce read length N50 of 100 kb or higher, but it requires much more input DNA (~10 µg) with lower data yield. Another advantage of the Saphyr platform is that in addition to quantifying the copy number of D4Z4 repeat units, it will also enable the de novo assembly of a human genome and the genome-wide identification structural variants.[27] Therefore, optical mapping can serve a dual purpose of identifying structural variants that may be relevant to the phenotypic presentations in the patient, especially when FSHD diagnostic testing yields negative results.

Table 2 Analysis of Bionano Irys genome mapping data sets of three families

	ID	Ethnicity	Relationship	Irys optical mapping (Nb.BssSI enzyme)			Irys optical mapping (Nt.BspQI enzyme)		
				Units	Allele	Read count	Units	Allele	Read count
Family 1	HG00512	Southern Han Chinese	Father	19	4qA	3	19.8±0.5	4qB	7
				–	–		40.4±0.3	4qA	3
	HG00513	Southern Han Chinese	Mother	11	4qA	6	10.4±0.2	4qA	8
				–	–		33.1±0.3	4qA	11
	HG00514	Southern Han Chinese	Daughter	11	4qA	6	10.6±0.2	4qA	9
				19	4qA	5	19.6±0.3	4qA	10
Family 2	HG00731	Puerto Rican	Father	20	4qB	5	19.9±0.5	4qB	7
				40	4qA	3	40.5±0.3	4qA	3
	HG00732	Puerto Rican	Mother	17	4qB	6	17.2±0.1	4qB	33
				32	4qB	4	32.1±0.3	4qB	18
	HG00733	Puerto Rican	Daughter	17	4qB	7	17.3±0.3	4qB	12
				40	4qA	2	40.1±0.4	4qA	7
Family 3	GM19238	Yorùbá	Mother	25	4qA	2	25.6±0.3	4qA	10
				–	–	–	49.1±0.7	4qA	13
	GM19239	Yorùbá	Father	9	4qB	5	9.2±0.1	4qB	14
				36	4qA	2	36.6±0.2	4qA	13
	GM19240	Yorùbá	Daughter	25	4qA	3	25.9±0.3	4qA	5
				36	4qA	4	36.2±0.4	4qA	7

We also recognise that there are several disadvantages of optical mapping, in comparison to conventional approaches such as Southern blot, in the contexts of molecular diagnosis of FSHD. First, although Southern blot may not be very accurate (especially for alleles with >17 repeats), for the purpose of molecular diagnosis, it can roughly tell the number and enable the diagnosis of FSHD when an allele with 1–10 repeat is observed. This straightforwardness may be one of the reasons for Southern blot to be commonly used for the diagnosis. Second, optical mapping is not yet cost-effective in comparison: there is an initial capital cost of a few hundred thousand dollars to establish the platform itself (including the computing hardware), and each subsequent flow cell currently costs ~US$500 even when purchased in batch. We note that it is possible to lower the cost in future versions of the flow cell by assaying >10 samples together (currently, it is limited to two samples), and that optical mapping can perform genome-wide survey of structural variants that may be relevant to disease diagnosis. Furthermore, although the Saphyr platform can run two human genomes in 1 day in an automated fashion (approximately ~300 Gb of data for each genome), the sample preparation itself takes approximately 1 day with extensive manual labour (see 'Materials and methods' section), and the data analysis and visualisation can take half a day. Southern blot-based diagnosis typically takes 1 week, but it has the clear advantage that >10 samples can be analysed on the same gel (and it is possible to run four gels in 1 week), allowing the simultaneous analysis of a large number of samples. Third, the number of reads encountered in optical mapping is highly size dependent, while this is not an issue using high-quality DNA (from agarose plugs) in a Southern blot; therefore, optical mapping may be less accurate when estimating the proportion of mosaicism when several alleles differ substantially in repeat counts.

There are several technical limitations of optical mapping that we wish to discuss here. First, our study focused on the molecular characterisation of patients with FSHD, and only included a very small number of unaffected control subjects. Currently, the average length of reads from the Saphyr platform is about 350 kb, even though the DNA molecules that were assayed in our study can range from 100 kb to over 1 Mb. Therefore, very long non-pathogenic D4Z4 repeats could not be accurately quantified by optical mapping. Indeed, if an allele has 50 units in control subjects, then the length of the repeat region would be 50×3.3 kb=165 kb; given that typical average size of an optical mapping is ~350 kb, many of the reads from optical mapping may not be able to cover the 'region of dissimilarity', so the effective coverage at the D4Z4 region will be much less than the genome-wide coverage (which is usually ~100× per flow cell). We illustrate the relationship between coverage and read length in online supplementary table 3: it is clear that samples with similar whole-genome coverage can vary greatly when focusing on longer reads: some samples such as P01 and P08 has very low effective coverage for reads >300 kb in comparison to other samples. This is not a problem for diagnosing FSHD per se, since <10 repeats are pathogenic, but it may pose a problem for population-scale analysis of D4Z4 repeats since it gives an upper bound of the number of repeats that can be detected by the platform. Second, for long-read platforms, there will be allelic biases where longer alleles tend to be present with lower number of reads than shorter alleles. Given the size distribution of all reads genome-wide calculated by the Bionano software, it is possible to estimate coverage biases of the two alleles. To further examine this issue, we have also compared the number of reads supporting shorter versus longer D4Z4 alleles for all subjects (online supplementary table 2). Except the 3 individuals with postzygotic mosaicism, among the 14 subjects, 5 have less reads covering the shorter alleles than the longer alleles; therefore, this potential bias does not appear to be a main concern. One reason why the length bias is not high may be due to the need to find very long flanking alignment around the D4Z4 repeats as shown in figure 2, so that the total length of aligned regions between the two alleles are comparable. Third, if there is complete deletion of the D4z4 array in an allele, then it will be hard to tell heterozygosity from homozygosity; in our samples we did not observe such events to evaluate this possibility, but they are likely to occur in the population. Fourth, the optical mapping is capable to distinguish 4qA-L from 4qB, but not from 4qA. To the best of our knowledge, there is little clinical implication whether

4qA-L or 4qA is present,[28] since they both show phenotypes of FSHD when repeat number is 1–10. We note that the GRCh38.p7 release also includes KQ983258.1 as patch scaffold providing representation for the variant 4qA-L haplotype, which is slightly (~1.6 kb) longer than the 4qA haplotype.

We also wish to discuss several limitations of the current study design. First, with the exception of patient P02 and P03 (offspring and mother), we were not able to obtain parental data for patients under the study. As previously reviewed,[29] several studies demonstrated that de novo repeat contraction may account for a surprisingly high percentage of FSHD patients (10%–33%),[30 31] and this high incidence can be partly explained by the presence of parental mosaicism for 4q short alleles that has been reported in 19% of de novo cases.[32 33] Lemmers et al[34] demonstrated that somatic mosaicism in FSHD patients goes largely undetected using the standard diagnostic technique, indicating that linear electrophoresis is unsuitable to identify mosaic patients, yet pulsed-field gel electrophoresis (PFGE)-based method can accurately reveal somatic mosaicism in patients and parents. Among the three patients with postzygotic mosaicism in our study (P04, P05 and P06), one of them (P05) had a family history of FSHD and a relatively late onset at age 31. Detailed examination of medical records showed that P05 was a female patient who was referred to the clinic due to mild symptoms and due to a confirmed diagnosis of an offspring with early onset FSHD. Note that we were unable to determine the genetic origin of the pathogenic mutation in P05 due to the lack of parental data; similarly, we were unable to determine whether the contracted repeat number differs between P05 and her offspring as the offspring did not consent in this study. Nevertheless, this case represented an interesting example where postzygotic mosaicism was inferred in a patient suspected to carry germline mosaicism, corroborating previous reports that a substantial fraction of mosaic parents with germline mosaicism in oogenesis may have been overlooked.[33] One additional limitation of the current study is that we used blood samples for molecular diagnosis, rather than muscle biopsy from affected areas. However, in practice, it is generally not feasible and not desirable to take a muscle biopsy for DNA analysis, therefore limiting our ability to compare results between blood and tissues in the current study. Expanding muscle-derived cells in vitro, such as satellite cells or induced pluripotent stem (iPS) cells, might be helpful in determining the degree of mosaicism in affected muscles.

In conclusion, we established the technical feasibility of using Bionano Genomics's Saphyr platform to perform molecular diagnosis of FSHD, and discussed a number of advantages, limitations and possible modifications that may improve the detection accuracy and reliability. With the ever decreasing cost of performing genome mapping on the single-molecule optical mapping platform, and the recent introduction of Direct Label and Stain technology, we expect that this method may be widely applied in research and clinical settings of FSHD, and may potentially expedite the genetic studies on this devastating disease. Lastly, this study may serve as a model, which demonstrated how the workflow can be applied to other rare diseases involving complex genomic structural changes.

Author affiliations
[1]Department of Neurology, Peking Union Medical College Hospital, Chinese Academy of Medical Sciences, Beijing, China
[2]GrandOmics Biosciences, Beijing, China
[3]Department of Neurology and Institute of Neurology, First Affiliated Hospital, Center of Neuroscience, Fujian Medical University, Fuzhou, China
[4]Raymond G. Perelman Center for Cellular and Molecular Therapeutics, Children's Hospital of Philadelphia, Philadelphia, Pennsylvania, USA
[5]Department of Pathology and Laboratory Medicine, University of Pennsylvania Perelman School of Medicine, Philadelphia, Pennsylvania, USA
[6]Department of Medical Genetics, School of Basic Medical Sciences, Peking University Health Science Center, Beijing, China
[7]Department of Medical Genetics, Peking Union Medical College Hospital, Chinese Academy of Medical Sciences, Beijing, China
[8]Neuroscience Center, Chinese Academy of Medical Sciences, Beijing, China, Beijing, China

ORCID iDs
Fan Yang http://orcid.org/0000-0003-1556-1436
Kai Wang http://orcid.org/0000-0002-5585-982X

REFERENCES

1. Cooper D, Upadhhyaya M, Dystrophy FM. (FSHD): Clinical Medicine and Molecular Cell Biology. Abingdon, UK: Garland Science/BIOS Scientific Publishers, 2004.
2. Padberg GW, Brouwer OF, de Keizer RJ, Dijkman G, Wijmenga C, Grote JJ, Frants RR. On the significance of retinal vascular disease and hearing loss in facioscapulohumeral muscular dystrophy. Muscle Nerve Suppl 1995;2:S73–80.
3. Saito Y, Miyashita S, Yokoyama A, Komaki H, Seki A, Maegaki Y, Ohno K. Facioscapulohumeral muscular dystrophy with severe mental retardation and epilepsy. Brain Dev 2007;29:231–3.
4. Deenen JCW, Arnts H, van der Maarel SM, Padberg GW, Verschuuren JJGM, Bakker E, Weinreich SS, Verbeek ALM, van Engelen BGM. Population-Based incidence and prevalence of facioscapulohumeral dystrophy. Neurology 2014;83:1056–9.
5. Lyle R, Wright TJ, Clark LN, Hewitt JE. The FSHD-associated repeat, D4Z4, is a member of a dispersed family of homeobox-containing repeats, subsets of which are clustered on the short arms of the acrocentric chromosomes. Genomics 1995;28:389–97.
6. Winokur ST, Bengtsson U, Vargas JC, Wasmuth JJ, Altherr MR, Weiffenbach B, Jacobsen SJ. The evolutionary distribution and structural organization of the homeobox-containing repeat D4Z4 indicates a functional role for the ancestral copy in the FSHD region. Hum Mol Genet 1996;5:1567–75.
7. Hewitt JE, Lyle R, Clark LN, Valleley EM, Wright TJ, Wijmenga C, van Deutekom JC, Francis F, Sharpe PT, Hofker M, Frants RR, Williamson R. Analysis of the tandem repeat locus D4Z4 associated with facioscapulohumeral muscular dystrophy. Hum Mol Genet 1994;3:1287–95.
8. Ding H, Beckers MC, Plaisance S, Marynen P, Collen D, Belayew A. Characterization of a double homeodomain protein (DUX1) encoded by a cDNA homologous to 3.3 kb dispersed repeated elements. Hum Mol Genet 1998;7:1681–94.
9. van Geel M, Dickson MC, Beck AF, Bolland DJ, Frants RR, van der Maarel SM, de Jong PJ, Hewitt JE. Genomic analysis of human chromosome 10q and 4q telomeres suggests a common origin. Genomics 2002;79:210–7.

Methods

10. Lemmers RJLF, de Kievit P, Sandkuijl L, Padberg GW, van Ommen G-JB, Frants RR, van der Maarel SM. Facioscapulohumeral muscular dystrophy is uniquely associated with one of the two variants of the 4q subtelomere. *Nat Genet* 2002;32:235–6.

11. Lemmers RJLF, van der Vliet PJ, Klooster R, Sacconi S, Camaño P, Dauwerse JG, Snider L, Straasheijm KR, van Ommen GJ, Padberg GW, Miller DG, Tapscott SJ, Tawil R, Frants RR, van der Maarel SM. A unifying genetic model for facioscapulohumeral muscular dystrophy. *Science* 2010;329:1650–3.

12. Lemmers RJLF, Tawil R, Petek LM, Balog J, Block GJ, Santen GWE, Amell AM, van der Vliet PJ, Almomani R, Straasheijm KR, Krom YD, Klooster R, Sun Y, den Dunnen JT, Helmer Q, Donlin-Smith CM, Padberg GW, van Engelen BGM, de Greef JC, Aartsma-Rus AM, Frants RR, de Visser M, Desnuelle C, Sacconi S, Filippova GN, Bakker B, Bamshad MJ, Tapscott SJ, Miller DG, van der Maarel SM. Digenic inheritance of an SMCHD1 mutation and an FSHD-permissive D4Z4 allele causes facioscapulohumeral muscular dystrophy type 2. *Nat Genet* 2012;44:1370–4.

13. Gatica LV, Rosa AL. A complex interplay of genetic and epigenetic events leads to abnormal expression of the DUX4 gene in facioscapulohumeral muscular dystrophy. *Neuromuscul Disord* 2016;26:844–52.

14. van der Maarel SM, Deidda G, Lemmers RJ, Bakker E, van der Wielen MJ, Sandkuijl L, Hewitt JE, Padberg GW, Frants RR. A new dosage test for subtelomeric 4;10 translocations improves conventional diagnosis of facioscapulohumeral muscular dystrophy (FSHD). *J Med Genet* 1999;36:823–8.

15. Lemmers RJL, de Kievit P, van Geel M, van der Wielen MJ, Bakker E, Padberg GW, Frants RR, van der Maarel SM. Complete allele information in the diagnosis of facioscapulohumeral muscular dystrophy by triple DNA analysis. *Ann Neurol* 2001;50:816–9.

16. Nguyen K, Puppo F, Roche S, Gaillard M-C, Chaix C, Lagarde A, Pierret M, Vovan C, Olschwang S, Salort-Campana E, Attarian S, Bartoli M, Bernard R, Magdinier F, Levy N. Molecular combing reveals complex 4q35 rearrangements in facioscapulohumeral dystrophy. *Hum Mutat* 2017;38:1432–41.

17. Vasale J, Boyar F, Jocson M, Sulcova V, Chan P, Liaquat K, Hoffman C, Meservey M, Chang I, Tsao D, Hensley K, Liu Y, Owen R, Braastad C, Sun W, Walrafen P, Komatsu J, Wang J-C, Bensimon A, Anguiano A, Jaremko M, Wang Z, Batish S, Strom C, Higgins J. Molecular combing compared to southern blot for measuring D4Z4 contractions in FSHD. *Neuromuscul Disord* 2015;25:945–51.

18. Morioka MS, Kitazume M, Osaki K, Wood J, Tanaka Y. Filling in the gap of human chromosome 4: single molecule real time sequencing of Macrosatellite repeats in the facioscapulohumeral muscular dystrophy locus. *PLoS One* 2016;11:e0151963.

19. Mitsuhashi S, Nakagawa S, Takahashi Ueda M, Imanishi T, Frith MC, Mitsuhashi H. Nanopore-based single molecule sequencing of the D4Z4 array responsible for facioscapulohumeral muscular dystrophy. *Sci Rep* 2017;7:14789.

20. Lam ET, Hastie A, Lin C, Ehrlich D, Das SK, Austin MD, Deshpande P, Cao H, Nagarajan N, Xiao M, Kwok P-Y. Genome mapping on nanochannel arrays for structural variation analysis and sequence assembly. *Nat Biotechnol* 2012;30:771–6.

21. Barseghyan H, Tang W, Wang RT, Almalvez M, Segura E, Bramble MS, Lipson A, Douine ED, Lee H, Délot EC, Nelson SF, Vilain E. Next-Generation mapping: a novel approach for detection of pathogenic structural variants with a potential utility in clinical diagnosis. *Genome Med* 2017;9:90.

22. Wang Z-Q, Wang N, van der Maarel S, Murong S-X, Wu Z-Y. Distinguishing the 4qA and 4qB variants is essential for the diagnosis of facioscapulohumeral muscular dystrophy in the Chinese population. *Eur J Hum Genet* 2011;19:64–9.

23. Lee JH, Goto K, Matsuda C, Arahata K. Characterization of a tandemly repeated 3.3-kb KpnI unit in the facioscapulohumeral muscular dystrophy (FSHD) gene region on chromosome 4q35. *Muscle Nerve Suppl* 1995;2:S6–13.

24. Hastie A, Pang AW, Lee J, Lam ET, Anantharaman T, Andrews W, Saghbini M, Cao H. Next-Generation mapping: a highly sensitive and accurate method for interrogation of clinically relevant structural variation. American Society of Human Genetics Annual Meeting. Vancouver, Canader, 2016.

25. Schwartz DC, Li X, Hernandez LI, Ramnarain SP, Huff EJ, Wang YK. Ordered restriction maps of Saccharomyces cerevisiae chromosomes constructed by optical mapping. *Science* 1993;262:110–4.

26. Zhang Q, Xu X, Ding L, Li H, Xu C, Gong Y, Liu Y, Mu T, Leigh D, Cram DS, Tang S. Clinical application of single-molecule optical mapping to a multigeneration FSHD1 pedigree. *Mol Genet Genomic Med* 2019;7:e565.

27. Mak ACY, Lai YYY, Lam ET, Kwok T-P, Leung AKY, Poon A, Mostovoy Y, Hastie AR, Stedman W, Anantharaman T, Andrews W, Zhou X, Pang AWC, Dai H, Chu C, Lin C, Wu JJK, Li CML, Li J-W, Yim AKY, Chan S, Sibert J, Džakula Željko, Cao H, Yiu S-M, Chan T-F, Yip KY, Xiao M, Kwok P-Y. Genome-Wide structural variation detection by genome mapping on Nanochannel arrays. *Genetics* 2016;202:351–62.

28. Lemmers RJ, van der Vliet PJ, Balog J, Goeman JJ, Arindrarto W, Krom YD, Straasheijm KR, Debipersad RD, Özel G, Sowden J, Snider L, Mul K, Sacconi S, van Engelen B, Tapscott SJ, Tawil R, van der Maarel SM. Deep characterization of a common D4Z4 variant identifies biallelic DUX4 expression as a modifier for disease penetrance in FSHD2. *Eur J Hum Genet* 2018;26:94–106.

29. Ricci G, Zatz M, Tupler R. Facioscapulohumeral muscular dystrophy: more complex than it appears. *Curr Mol Med* 2014;14:1052–68.

30. Zatz M, Marie SK, Passos-Bueno MR, Vainzof M, Campiotto S, Cerqueira A, Wijmenga C, Padberg G, Frants R. High proportion of new mutations and possible anticipation in Brazilian facioscapulohumeral muscular dystrophy families. *Am J Hum Genet* 1995;56:99–105.

31. Padberg GW, Frants RR, Brouwer OF, Wijmenga C, Bakker E, Sandkuijl LA. Facioscapulohumeral muscular dystrophy in the Dutch population. *Muscle Nerve Suppl* 1995;2:S81–4.

32. Upadhyaya M, Maynard J, Osborn M, Jardine P, Harper PS, Lunt P. Germinal mosaicism in facioscapulohumeral muscular dystrophy (FSHD). *Muscle Nerve Suppl* 1995;2:S45–9.

33. Köhler J, Rupilius B, Otto M, Bathke K, Koch MC. Germline mosaicism in 4q35 facioscapulohumeral muscular dystrophy (FSHD1A) occurring predominantly in oogenesis. *Hum Genet* 1996;98:485–90.

34. Lemmers RJLF, van der Wielen MJR, Bakker E, Padberg GW, Frants RR, van der Maarel SM. Somatic mosaicism in FSHD often goes undetected. *Ann Neurol* 2004;55:845–50.